

Analysis of Fundus Image of Ophthalmoscope for Macula Identification and Detection to Diagnosis of Vision Related Diseases – by Gray Thresholding and Pixel Index Number

Vaishali B. Shinde
Dept. of Computer Science & IT
Dr. B. A. M. University, Aurangabad

Ramesh R. Manza
Dept. of Computer Science & IT
Dr. B. A. M. University, Aurangabad

ABSTRACT

As we know the diabetic causes people are increasing day by day in the world. Diabetic disease has also infects the other parts of the human body, like eye, platelets counts etc. In the field of medicines, medical image processing plays a vital role to detect the abnormalities of eye or eye diseases like glaucoma and diabetic retinopathy. Macular degeneration is one of the medical conditions that affect the vision of elder people [1]. The retina is responsible for peripheral vision. Macula is the central area of the retina, temporal to the optic disk. It is responsible to have fine central vision and colour vision. This paper provides the Manual analysis of the images can be improved and problem of detection diabetics by identifying and detecting macula using gray thresholding and index number of object.

General Terms

Ophthalmology engines

Keywords

Macula, Graythresh, Index Number

1. INTRODUCTION

Diabetic disease has also infects the other parts of the human body, like eye, platelets counts etc. In the field of medicines, medical image processing plays a vital role to detect the abnormalities of eye or eye diseases like glaucoma and diabetic retinopathy. Macular degeneration is one of the medical conditions that affect the vision of elder people [1]. The retina is responsible for peripheral vision. Macula is the central area of the retina, temporal to the optic disk. It is responsible to have fine central vision and colour vision. With macular degeneration, a scotoma, an isolated retinal area of diminished vision, may appear in the central visual field. The visual system of a person with a central scotoma from a sensory default is thought to choose a preferred eccentric retinal area to perform the visual tasks that the nonfunctioning fovea used to perform. [2]. In ophthalmology, for diagnosis of diabetes, digital colour retinal images are becoming increasingly important. In computer based retinal image analysis system, image processing techniques are used in order to facilitate and improve diagnosis. Manual analysis of the images can be improved and problem of detection of diabetes in the late stage for optimal treatment may be resolved. The Image Ret database was made publicly available in 2008 and is subdivided into two sub-databases, DIARETDB0 and DIARETDB1 [3]. DIARETDB0 contains 130 retinal images of which 20 are normal and 110 contain various symptoms of diabetic retinopathy. The World Health

Organization estimates that 135 million people have diabetes mellitus worldwide and that the number of people with diabetes will increase to 300 million by the year 2025 [4].

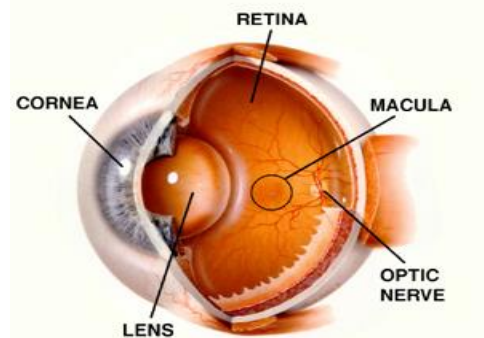


Figure 1. Eye Anatomy

2. LITERATURE SURVEY

Ziyang Liang et al [5] presents a method of detecting drusen in retinal fundus images. The method first determines the location of the macula, which is used as a landmark for a clinical drusen grading overlay. Subsequently, regions of drusen are identified through maximal region-based pixel intensity approaches via RGB and HSV channels. Methods of reducing the effect of retinal and choroidal vessels are also described. The system is tested on a sample set of 16 fundus images from a clinical study, with half having drusen. Experiments on the results show a sensitivity and specificity of 0.75 on the test image set. Wong, D.W.K. et al [6]. This paper, presented an approach to automatically determine the macula centre in retinal fundus images. First contextual information on the image is combined with a statistical model to obtain an approximate macula region of interest localization. Subsequently, it proposes the use of a seeded mode tracking technique to locate the macula centre. The proposed approach is tested on a large dataset composed of 482 normal images and 162 glaucoma images from the ORIGA database and an additional 96 AMD images. The results show a ROI detection of 97.5% and 90.5% correct detection of the macula within 1/3DD from a manual reference, which outperforms other current methods. Shijian Lu et al [7] describes an automatic macula detection technique that makes use of the circular brightness profile of the macula: A line operator is designed to capture the macula

circular brightness profile, which evaluates the image brightness variation along multiple line segments of specific orientations that pass through each retinal image pixel. The orientation of the line segment with the minimum/ maximum variation has specific patterns that indicate the position of the macula efficiently. The proposed technique has been tested over DRIVE project's dataset and the STARE project's dataset. Experiments show that the accuracies reach up to 100% and 95.45%, respectively, based on 35 and 44 retinal images having discernible macula within the two public datasets. Tobin et al [8] present results for the automatic detection of the optic nerve and localization of the macula using digital red-free fundus photography. This method relies on the accurate segmentation of the vasculature of the retina followed by the determination of spatial features describing the density, average thickness, and average orientation of the vasculature in relation to the position of the optic nerve. Localization of the macula follows using knowledge of the optic nerve location to detect the horizontal raphe of the retina using a geometric model of the vasculature. Authors report 90.4% detection performance for the optic nerve and 92.5% localization performance for the macula for red-free fundus images representing a population of 345 images corresponding to 269 patients with 18 different pathologies associated with DR and other common retinal diseases such as age-related macular degeneration. Liu et al [9] The ratio of the optic cup to disc (CDR) in retinal fundus images is one of the principal physiological characteristics in the diagnosis of glaucoma. Currently the CDR is manually determined which can be subjective and limits its use in mass screening. To automatically extract the disc, a variational level set method is proposed in this paper. For the cup, two methods making use of color intensity and threshold level set are evaluated. A batch of 73 retinal images from the Singapore Eye Research Centre was used to assess the performance of the determined CDR to the clinical CDR, and it was found that the threshold and variational level set methods produced 97% accuracy in the determined CDR results, an 18% improvement over the color intensity method. The results indicate potential applicability of the methods for automated and objective mass screening for early detection of glaucoma. Veras et al [10] Fundus images are valuable resource in diagnosis because they often present indications about retinal, ophthalmic, and even systemic diseases such as diabetes, hypertension, and arteriosclerosis. Processing and analysis. The method makes use of the optic disc height obtained from the ARGALI to define the region of interest. Regions of dark spots are then detected by finding the coordinates with the lowest pixel intensity and determining the average pixel neighbourhood intensities. These regions are ranked to determine the region containing the macula. This algorithm was tested on 162 images, and an accuracy of 98.8% was achieved. The results are promising for further development and use of this method in AMD studies and physiology localization.

3. PROPOSED METHOD

To diagnosis vision related diseases, it is important to identify and detect the macula and their region. The blood vessels are arising from optic disk to macula that is on temporal side of optic disk. The ruptured blood vessels, the clotting of blood, block of vein and cut blood vessels are easily identified with the help of macula. In the research, the aim is to diagnose vision related diseases by identifying and detecting the macula.

3.1 Methodology

This section discusses some of the principles applied in this research work. Key issues to pursue in order to improve algorithmic performance are to explore the physical properties of retinal objects on retinal images and to relate these to our algorithm design and performance analysis. These principles include: Extracting green channel, Histogram Equalization, Image Morphological Operations and Graythresholding and macula detection.

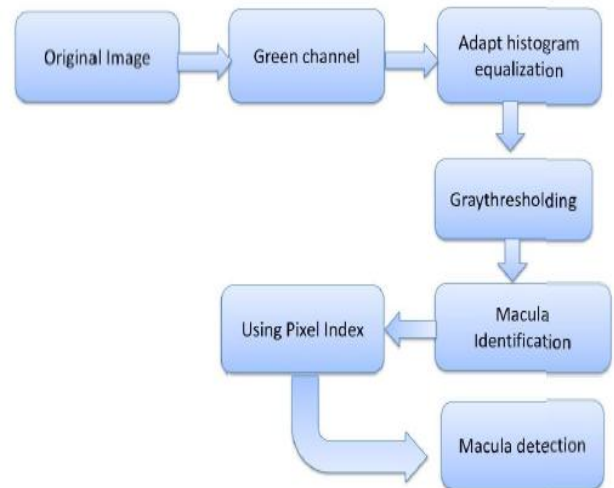


Figure 2. Methodology of system

3.2 Macula Identification and Detection

3.2.1 Adaptive Histogram Equalization

This section proceeds with a concise mathematical description of AHE which can be readily generalized, and then considers the two main types of modification. The relationship between the equations and different (conceptual) perspectives on AHE, such as GL comparison, might not be immediately clear, but generalizations can be expressed far more easily in this framework.

To equalize an input image with quantized GL's scaled between $-1/2$ and $1/2$, we first require an estimate $h\Lambda$ of the local histogram. (Some implementations do not actually evaluate any histograms, but can be said to do so implicitly.) We can start by sifting those pixels in the input image with GL q using the Kronecker delta function $\delta(i,j)$, which equals 1 if $i=j$ and 0 otherwise. Spatial convolution with a rectangular kernel fw can then be used to find the number of such pixels in a window around each point. It is convenient to scale fw so that it is unit-volume; the estimate histogram then sums to unity at each point. For a square window of width w , with odd-integer value, this can be written

$$\hat{h}(m, n, g) = \delta(g, x(m, n)) \star_{m, n} fw(m, n) \quad (1)$$

$$fw(m, n) = \begin{cases} w^{-2}, & |m| \leq \frac{w-1}{2} \\ 0, & \text{otherwise} \end{cases} \dots\dots(2)$$

The output image y is found using

$$y(m, n) = z(m, n) \dots\dots\dots(3)$$

where z is a spatially varying mapping. In standard HE, the cumulative histogram is used for this. Because sums to unity, z can be constructed using an offset of $1/2$ so that the output ranges from $-1/2$ to $1/2$. We add a third term so that negating the input GL values negates the output:

$$z(m, n, g) = -1/2 + \sum_{\gamma < g} \hat{h}(m, n, \gamma) + \dots$$

$$= 1/2 + \sum_{\gamma < g} \hat{h}(m, n, \gamma) - \frac{1}{2} \sum_{\gamma < g} \dots \dots \dots (4)$$

This can be generalized using what we call a “cumulation function”, f_c

$$z(m, n, g) = \sum_{\gamma} \hat{h}(m, n, \gamma) f_c \dots \dots \dots (5)$$

In standard HE, only operates on GL differences

$$f_c(\mu, \theta) \dots \dots \dots (6)$$

$$f_0(d) = \sum \dots \dots \dots (7)$$

The limit B must be equal to, or greater than, the maximum GL difference. (This limit is exploited in the Fourier series implementation of HE, which employs a periodic cumulation function.) Alternatively, can be described using convolution over

$$z(m, n, g) = \hat{h}(m, n, g) \dots \dots \dots (8)$$

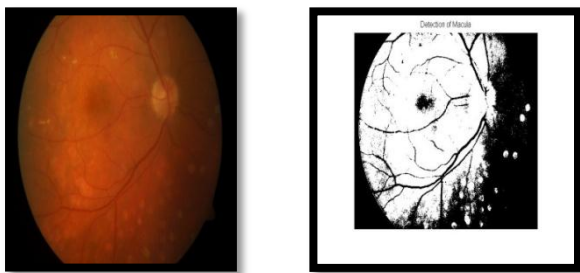


Figure 3 Original Image Result of Adaptive Histogram Equalization

3.2.2 Gray Thresholding

Thresholding is a technique frequently applied to image segmentation. Its basic objective is to classify the pixels of a given image into two classes: those pertaining to an object and those pertaining to the background. For the image with clear objects in the background, the bi-level thresholding method can easily divide the object from the background.

Single (bi-level) or multiple thresholding is a straightforward and effective technique for image segmentation and computer vision. However, it requires an adequate threshold value to extract objects of interest from their background, since the objects in an image have their own distinct gray-level distributions. Thresholding is widely used in many image processing applications.

The number of pixels at level i is denoted by n_i and the total number of pixels by $N = n_1 + n_2 + \dots + n_L$. In order to simplify the discussion, the gray-level histogram is normalized and regarded as a probability distribution:

$$P_i = \frac{n_i}{N}, P_i \geq 0, \sum_{i=0}^L P_i = 1 \dots \dots \dots (1)$$

Now suppose that we dichotomize the pixels into two classes C_0 and C_1 (background and objects, or vice versa) by a threshold at level k ; C_0 denotes pixels with levels $[1, \dots, k]$, and C_1 denotes pixels with levels $[k + 1, \dots, L]$. Then the probabilities of class occurrence and the class mean levels, respectively, are given by

$$\omega_0 = \Pr(C_0) = \sum_{i=1}^k P_i = \omega(k) \dots \dots \dots (2)$$

$$\omega_1 = \Pr(C_1) = \sum_{i=k+1}^L P_i = 1 - \omega(k) \dots \dots \dots (3)$$

And

$$\mu_0 = \sum_{i=1}^k i \Pr(i | C_0) = \sum_{i=1}^k iP_i / \omega_0 = \mu(k) / \omega(k) \dots (4)$$

$$\mu_1 = \sum_{i=k+1}^L i \Pr(i | C_1) = \sum_{i=k+1}^L iP_i / \omega_1 = \frac{\mu_T - \mu(k)}{1 - \omega(k)}, \dots (5)$$

Where

$$\omega(k) = \sum_{i=1}^k P_i \dots \dots \dots (6)$$

and

$$\mu(k) = \sum_{i=1}^k iP_i \dots \dots \dots (7)$$

are the zeroth- and the first-order cumulative moments of the histogram up to the k^{th} level, respectively, and

$$\mu_T = \mu(L) = \sum_{i=1}^L iP_i \dots \dots \dots (8)$$

is the total mean level of the original picture. We can easily verify the following relation for any choice of k :

$$\omega_0 \mu_0 + \omega_1 \mu_1 = \mu_T, \quad \omega_0 + \omega_1 = 1 \dots \dots \dots (9)$$

The class variances are given by

$$\sigma_0^2 = \sum_{i=1}^k (i - \mu_0)^2 \Pr(i | C_0) = \sum_{i=1}^k (i - \mu_0)^2 P_i / \omega_0 \dots (10)$$

$$\sigma_1^2 = \sum_{i=k+1}^L (i - \mu_1)^2 \Pr(i | C_1) = \sum_{i=k+1}^L (i - \mu_1)^2 P_i / \omega_1 \dots (11)$$

These require second-order cumulative moments (statistics). In order to evaluate the "goodness" of the threshold (at level k), we shall introduce the following discriminate criterion measures (or measures of class separability) used in the discriminate analysis [5]:

$$\lambda = \frac{\sigma_B^2}{\sigma_W^2}, K = \frac{\sigma_T^2}{\sigma_W^2}, \eta = \frac{\sigma_B^2}{\sigma_T^2}, \dots \dots \dots (12)$$

where

$$\sigma_W^2 = \omega_0 \sigma_0^2 + \omega_1 \sigma_1^2 \dots \dots \dots (13)$$

$$\sigma_B^2 = \omega_0 (\mu_0 - \mu_T)^2 + \omega_1 (\mu_1 - \mu_T)^2 = \omega_0 \omega_1 (\mu_1 - \mu_0)^2 \dots \dots \dots (14)$$

(due to (9)) and

$$\sigma_T^2 = \sum_{i=1}^L (i - \mu_T)^2 P_i \dots \dots \dots (15)$$

are the within-class variance, the between-class variance, and the total variance of levels, respectively. Then our problem is reduced to an optimization problem to search for a threshold k that maximizes one of the object functions (the criterion measures) in (12). This standpoint is motivated by a conjecture that well threshold classes would be separated in gray levels, and conversely, a threshold giving the best separation of classes in gray levels would be the best threshold.

The discriminate criteria maximizing A , K , and q , respectively, for k are, however, equivalent to one another; e.g., $K = i + 1$ and $=)/(2 + 1)$ in terms of 2, because the following basic relation always holds:

$$\sigma_W^2 + \sigma_B^2 = \sigma_T^2 \dots\dots\dots(16)$$

It is noticed that σ_B^2 and q are functions of threshold level k , but σ_T^2 is independent of k . It is also noted that σ_B^2 is based on the second-order statistics (class variances), while q is based on the first-order statistics (class means). Therefore, q is the simplest measure with respect to k . Thus we adopt q as the criterion measure to evaluate the "goodness" (or separability) of the threshold at level k .

The optimal threshold k^* that maximizes q , or equivalently maximizes σ_B^2 is selected in the following sequential search by 6 using the simple cumulative quantities (6) and (7), or explicitly (6) using (2)-(5):

$$\eta(k) = \frac{\sigma_B^2(k)}{\sigma_T^2} \dots\dots\dots(17)$$

$$\sigma_B^2(k) = \frac{[\mu_T \omega(k) - \mu(k)]^2}{\omega(k)[1 - \omega(k)]} \dots\dots\dots(18)$$

and the optimal threshold k^* is

$$\sigma_B^2(k^*) = \max_{1 \leq k \leq L} \sigma_B^2(k) \dots\dots\dots(19)$$

From the problem, the range of k over which the maximum is sought can be restricted to

$$S^* = \{k; \omega_0 \omega_1 = \omega(k)[1 - \omega(k)] > 0, \text{ or } 0 < \omega(k) < 1\}$$

We shall call it the effective range of the gray-level histogram. From the definition in (14), the criterion measure σ_B^2 (or q) takes a minimum value of zero for such k as $k \in S - S^* = \{k; \omega(k) = 0 \text{ or } 1\}$ (i.e., making all pixels either CI or CO, which is, of course, not our concern) and takes a positive and bounded value for $k \in S^*$. It is, therefore, obvious that the maximum always exists.

3.2.3 Pixel Index Number for Detecting Macula

By checking manually, number from 1 to 28 to detect macula from image. From database, all images have different pixel index number. From all the pixel index

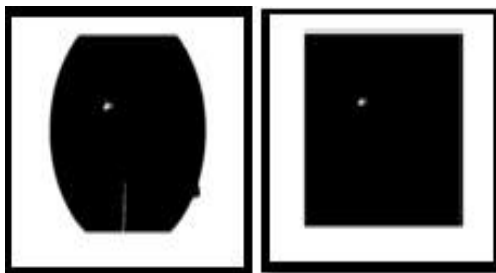


Figure 4 Result of AHE & Macula Identifying



Figure5 Identifying Macula & Detection Macula

4. RESULT

Calculating Morphology of Macula Using Pixel Index number.

Table 1. Area, Centroid and BoundingBox of macula from image001-image010

Sr. no	Image no.	Index no.	Area	Centroid	Bounding Box
1	Image001	3	1	285 580	284.5000 579.5000 1.0000 1.0000
2	Image002	5	1	394 206	393.5000 205.5000 1.0000 1.0000
3	Image003	2	1742	323.5534 553.3611	213.5000 520.5000 198.0000 61.0000
4	Image004	23	2208	915.9429 720.6332	877.5000 693.5000 82.0000 53.0000
5	Image005	8	188	398.6543 160.1383	390.5000 139.5000 16.0000 41.0000
6	Image006	16	99	615.3030 351.5354	605.5000 337.5000 18.0000 28.0000
7	Image007	6	182	382.5220 205.9396	366.5000 199.5000 33.0000 13.0000
8	Image008	40	6	1.0e+03 * 1.4045 0.7970	1.0e+03 * 1.4035 0.7955 0.0020 0.0030
9	Image009	11	1	412 263	411.5000 262.5000 1.0000 1.0000
10	Image010	11	1	412 263	411.5000 262.5000 1.0000 1.0000

The Image Ret database was made publicly available in 2008 and is subdivided into two sub-databases, DIARETDB0 and DIARETDB1 [18]. DIARETDB0 contains 130 retinal images of which 20 are normal and 110 contain various symptoms of diabetic retinopathy. Out of 110 images 104 images are detected macula and calculating Area, Centroid and BoundingBox of each macula from the images. Accuracy of system is 94.5454 that are approximately 95%.

5. CONCLUSION

A novel system for the automatic identification and detection macula using gray thresholding and pixel index number has been proposed in this paper. Accuracy of the system has been evaluated on a database of 104 images. The results are encouraging and these methods contribute to our overall goal of development of a system for the automated screening of Diabetic Retinopathy in medical camps. Our research work is continuing to differentiate, different type's diabetic diseases with their names using pixel index number. Our future work will focus on prediction of DR in patients based on the changes in the caliber of retinal blood vessels.

6. ACKNOWLEDGMENTS

We are very much thankful to Department of Computer Science and IT, Dr. Babasaheb Ambedkar Marathwada University who assist in lot of ample to complete this work.

7. REFERENCES

- [1] Shinde Vaishali, R.R.manza," Analysis of Fundus Image of Ophthalmoscope for Macula Identification and Detection to Diagnosis of Vision Related Diseases – A Review", RTCST 2014 International Conference, August 2014.
- [2] Zhiheng Xu, Ronald SchuchardDavid Ross, Paul Benkeser. Tracking retinal motion with a scanning laser ophthalmoscope.In *Journal of Rehabilitation Research And Development*. volume 42 number 3, Pages 373 — 380 2005.
- [3] Eye Diseases Prevalence Research Group. Prevalence of age-related macular degeneration in the united states. *Arch Ophthalmol*. 2004 Apr;122(4):564–572. [PubMed]
- [4] A. F. Amos, D. J. McCarty, and P. Zimmet, "The rising global burden of diabetes and its complications: estimates and projections to the year 2010," *Diabetic Med*, vol. 14, pp. S57-85, 1997.
- [5] Ziyang Liang; Wong, D. W K; Jiang Liu; Kap-Luk Chan; Tien Yin Wong, "Towards automatic detection of age-related macular degeneration in retinal fundus images," *Engineering in Medicine and Biology Society (EMBC), 2010 Annual International Conference of the IEEE* , vol., no., pp.4100,4103, Aug. 31 2010-Sept. 4 2010
- [6] Wong, D.W.K.; Jiang Liu; Ngan-Meng Tan; Fengshou Yin; Xiangang Cheng; Ching-Yu Cheng; Cheung, G.C.M.; Tien Yin Wong, "Automatic detection of the macula in retinal fundus images using seeded mode tracking approach," *Engineering in Medicine and Biology Society (EMBC), 2012 Annual International Conference of the IEEE* , vol., no., pp.4950,4953, Aug. 28 2012-Sept. 1 2012
- [7] Shijian Lu; Joo Hwee Lim, "Automatic macula detection from retinal images by a line operator," *Image Processing (ICIP), 2010 17th IEEE International Conference on* , vol., no., pp.4073,4076, 26-29 Sept. 2010
- [8] Tobin, Kenneth W.; Chaum, Edward; Govindasamy, V.P.; Karnowski, T.P., "Detection of Anatomic Structures in Human Retinal Imagery," *Medical Imaging, IEEE Transactions on* , vol.26, no.12, pp.1729,1739, Dec. 2007
- [9] Liu, J.; Wong, D. W K; Lim, J.H.; Jia, X.; Yin, F.; Li, H.; Xiong, W.; Wong, T.Y., "Optic cup and disk extraction from retinal fundus images for determination of cup-to-disc ratio," *Industrial Electronics and Applications, 2008. ICIEA 2008. 3rd IEEE Conference on* , vol., no., pp.1828,1832, 3-5 June 2008
- [10] Veras, R.; Medeiros, F.; Silva, R.; Ushizima, D., "Assessing the accuracy of macula detection methods in retinal images," *Digital Signal Processing (DSP), 2013 18th International Conference on* , vol., no., pp.1,6, 1-3 July 2013
- [11] Tan, N.M.; Wong, D. W K; Liu, J.; Ng, W. J.; Zhang, Z.; Lim, J.H.; Tan, Z.; Tang, Y.; Li, H.; Lu, S.; Wong, T.Y., "Automatic detection of the macula in the retinal fundus image by detecting regions with low pixel intensity," *Biomedical and Pharmaceutical Engineering, 2009. ICBPE '09. International Conference on* , vol., no., pp.1,5, 2-4 Dec. 2009